LETTERS
PUBLISHED ONLINE: 14 DECEMBER 2008 | DOI: 10.1038/NPHYS1155
nature physics

Attosecond phase locking of harmonics emitted from laser-produced plasmas

Y. Nomura[1]*, R. Hörlein[1,2]*, P. Tzallas[3], B. Dromey[4], S. Rykovanov[1,5], Zs. Major[1], J. Osterhoff[1], S. Karsch[1], L. Veisz[1], M. Zepf[4], D. Charalambidis[3,6], F. Krausz[1,2] and G. D. Tsakiris[1]†

Laser-driven coherent extreme-ultraviolet (XUV) sources provide pulses lasting a few hundred attoseconds[1,2], enabling real-time access to dynamic changes of the electronic structure of matter[3,4], the fastest processes outside the atomic nucleus. These pulses, however, are typically rather weak. Exploiting the ultrahigh brilliance of accelerator-based XUV sources[5] and the unique time structure of their laser-based counterparts would open intriguing opportunities in ultrafast X-ray and high-field science, extending powerful nonlinear optical and pump–probe techniques towards X-ray frequencies, and paving the way towards unequalled radiation intensities. Relativistic laser–plasma interactions have been identified as a promising approach to achieve this goal[6–13]. Recent experiments confirmed that relativistically driven overdense plasmas are able to convert infrared laser light into harmonic XUV radiation with unparalleled efficiency, and demonstrated the scalability of the generation technique towards hard X-rays[14–19]. Here we show that the phases of the XUV harmonics emanating from the interaction processes are synchronized, and therefore enable attosecond temporal bunching. Along with the previous findings concerning energy conversion and recent advances in high-power laser technology, our experiment demonstrates the feasibility of confining unprecedented amounts of light energy to within less than one femtosecond.

The nonlinear response of matter exposed to intense femtosecond laser pulses gives rise to the emission of high-frequency radiation at harmonics of the laser oscillation frequency. If the harmonics are phase-locked, their superposition results in a train of attosecond bursts[20]. The concept has been so far successfully implemented in atomic gases[21], and culminated in isolated attosecond pulses by using few-cycle laser drivers[1,2]. The low generation efficiency of harmonic radiation from atoms has motivated research into alternative concepts. Dense, femtosecond-laser-produced plasmas hold promise of converting laser light into coherent harmonics with much higher efficiency and of exploiting much higher laser intensities, because the plasma medium—in contrast to the atomic emitters—imposes no restriction on the strength of the laser field driving the harmonics[6–13]. Recent experimental studies of harmonics produced from overdense plasmas impressively corroborate several theoretical predictions: the high conversion efficiency[19], the favourable scalability of the generation technique towards high photon energies[14,16,19] and excellent divergence due to the spatial coherence of the generated harmonics[19,22]. Whether the high-order harmonics that are produced in overdense plasmas possess the phase synchronism necessary for attosecond bunching of the produced radiation has lacked experimental evidence up to now. In this work we demonstrate that this is indeed the case and hence the door is open for the generation of attosecond XUV pulses many orders of magnitude more intense than available at present.

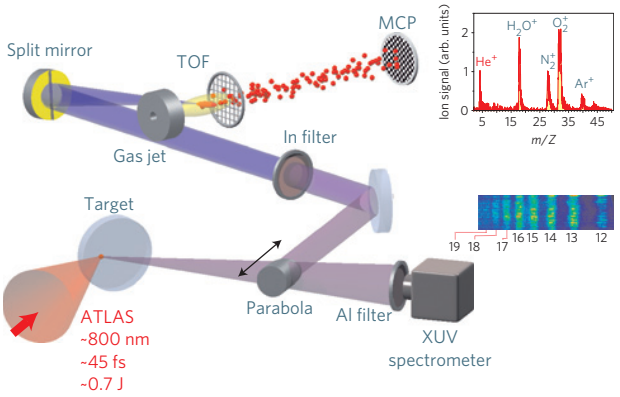

Figure 1 | Schematic diagram of the experimental set-up for the harmonic generation and its temporal characterization. The light reflected off the target into the specular direction is recollimated by a 25.4-mm-diameter 90° gold-coated off-axis parabolic mirror with the same focal length as the laser focusing parabola. The recollimating mirror is mounted on a flipper stage for easy withdrawal, thus enabling the spectral characterization of the emitted XUV light. Thin metal filters (typically 150 nm Al, In or Sn) inserted in front of the spectrometer provide a spectral preselection and block the laser light. With the recollimating parabolic mirror in place, the beam is deflected towards a 120-mm-diameter glass plate positioned at 60° angle of incidence. The reflection off the glass plate close to Brewster's angle (~57°) suppresses the *p*-polarized infrared laser light while reflecting a substantial fraction (~5% in *p* polarization) of the XUV harmonic emission. The 150 nm In filter selects harmonics from H8 to H14 and suppresses the residual laser light. This harmonic composition is focused into the He jet by a 300-mm-radius-of-curvature spherical mirror split into two halves, serving as a focusing wavefront divider. The generated ions are detected using a time-of-flight (TOF) spectrometer and a multichannel-plate (MCP) detector. The insets show raw data of a typical mass (upper) and harmonic (lower) spectrum.

Efficient harmonic generation from laser-produced plasmas relies on field strengths that result in values of the vector potential $a_L = |e|A_L/mc = \sqrt{I_L\lambda_L^2/(1.37\times10^{18}\,\mathrm{W\,\mu m^2\,cm^{-2}})}$ close

[1]Max-Planck-Institut für Quantenoptik, Hans-Kopfermann-Straße 1, D-85748 Garching, Germany, [2]Department für Physik, Ludwig-Maximilians-Universität, Am Coulombwall 1, D-85748 Garching, Germany, [3]Foundation for Research and Technology-Hellas, Institute of Electronic Structure & Laser, PO Box 1527, GR-711 10 Heraklion (Crete), Greece, [4]Department of Physics and Astronomy, Queens University Belfast, BT7 1NN, UK, [5]Moscow Physics Engineering Institute, Kashirskoe shosse 31, 115409 Moscow, Russia, [6]Department of Physics, University of Crete, PO Box 2208, GR-71003 Voutes-Heraklion (Crete), Greece. *These authors contributed equally to this work. †e-mail: george.tsakiris@mpq.mpg.de.

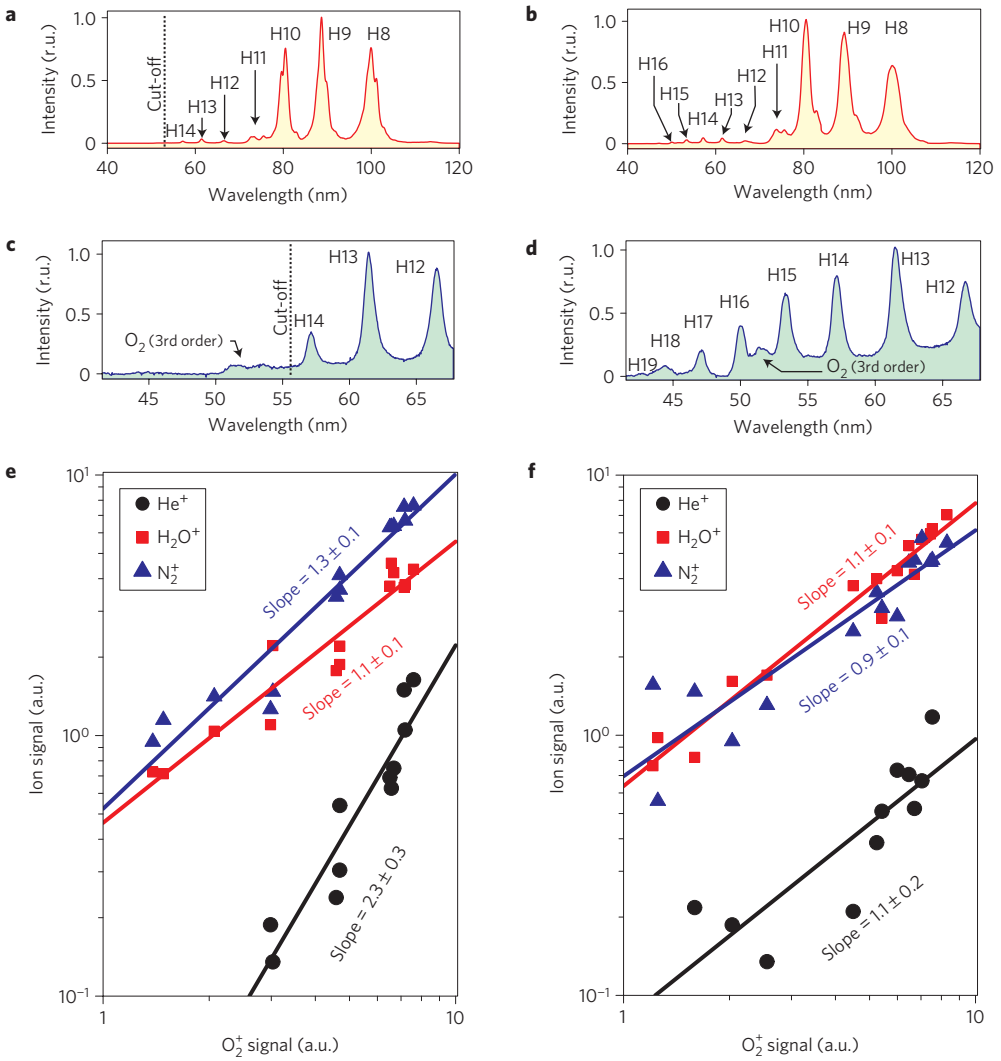

Figure 2 | Outline of the harmonic spectra and ion-yield dependence on the XUV radiation intensity for two target materials. a,**c**,**e**, Low-density (PMMA density ~1.2 g cm^{-3}) target; **b**,**d**,**f**, high density (glass density ~2.6 g cm^{-3}) target. The spectra shown in **a** and **b** have been filtered with a 150 nm In filter, whereas those in **c** and **d** with a 150 nm Al filter transmitting all harmonics above H10. In these panels a spurious signal due to third-order diffraction of O_2 line emission (~17 nm) is visible. As seen in **a** and **c**, the low-density target clearly shows the high-frequency cut-off at H14. By contrast, the spectrum in **d**, from the high-density target taken with the Al filter, extends to H19. **e**,**f**, The corresponding ion yields of various species (including those from the background gas) due to the harmonic composition shown in **a** and **b** against the O_2^+ yield. The dependence with slope ~1 indicates single-photon ionization whereas that with slope ~2 is evidence of two-photon ionization. The O_2^+ signal is proportional to the total XUV pulse energy because it is ionized by a single photon of any harmonic in the composition.

to (or larger than) unity. Here e and m are the electron's charge and rest mass, respectively, c is the velocity of light and A_L, I_L and λ_L stand for the amplitude of the vector potential, the cycle-averaged intensity and the wavelength of the incident laser light. Two distinct mechanisms have been identified to give rise to XUV harmonic emission from overdense plasmas produced by femtosecond laser pulses incident on a solid surface. One is based on a relativistic Doppler upshift of the laser light reflected off the oscillating plasma surface, acting as a relativistic oscillating mirror (ROM; refs 6,7). The other originates from currents excited by fast electrons in the density ramp of the plasma–vacuum interface leading to what has been dubbed coherent wake emission (CWE; refs 15,17). CWE is dominant at sub- or moderately relativistic intensities[17,18] for $a_L < 1$, whereas ROM becomes more efficient for $a_L > 1$ and completely takes over in the highly relativistic regime[12,19], when $a_L \gg 1$. In the transitional range for $a_L \approx 1$, the two processes can coexist and which one of the two dominates depends sensitively on the shape and gradient of the plasma density profile[18].

Phase coherence of the emitted XUV harmonics necessary for attosecond temporal bunching has been predicted for both generation processes, but the generation mechanisms leading to it have completely different physical origins. CWE is produced by electrons that are first pulled out from the plasma by the electric-field component of the incident laser pulse perpendicular to the target to be hurled back into the plasma during the next half cycle, where they excite plasma oscillations. Through linear mode conversion these plasma oscillations decay into electromagnetic waves at harmonics of the fundamental laser frequency[23]. It is the subfemtosecond temporal confinement of the electrons' re-encounter in the plasma that presumably leads to attosecond pulse formation in this case. The emitted bursts are expected to carry a chirp because their different spectral components are radiated from slightly different depths in the density ramp of the plasma–vacuum interface. On the other hand, ROM harmonics are due to the relativistic Doppler frequency shift acquired by the wave back-reflected from the plasma surface oscillating at velocities close

to the speed of light. Attosecond confinement is expected at the highest emitted frequencies. This is because the maximum Doppler upshift is confined to a small fraction of the laser oscillation period near the instants when the oscillating plasma surface moves towards the impinging laser pulse at maximum velocity. At these moments, the emerging bursts are expected to carry negligible chirp. The superior phase-locking properties of high-order ROM harmonics have been investigated in the theoretical treatment of ref. 12 and verified by wavelet analysis of particle-in-cell simulation results[13]. More details of the harmonic synchronization in connection with the two generation mechanisms, including results of particle-in-cell simulations, are given in Supplementary Information.

To address the question of mutual coherence among XUV harmonics and the resulting attosecond pulse generation from overdense plasmas, we have chosen the method of XUV autocorrelation (AC), which has already been applied successfully to the temporal characterization of atomic harmonic emission[24–26] (for details, see the Methods section). The technique is demanding in itself, but its application to plasma harmonics presents a particularly formidable challenge. This is mainly because, in contrast to the well-collimated XUV beams from atomic harmonic sources, plasma harmonics are emitted in a large cone owing to the tight focusing required for achieving high intensities. Moreover, harmonic generation from solid targets requires an assembly providing an undisturbed surface for each laser shot at a relatively high repetition rate for data accumulation. The experimental set-up shown in Fig. 1 is the result of a compromise between maximum possible collection efficiency and best possible suppression of the fundamental and the harmonics higher than 15th order, both requirements being of critical importance for successful implementation of nonlinear XUV AC. In our experiments we draw on two-photon ionization of He as the nonlinear process, which has been thoroughly investigated previously[27], with the number of He^+ ions serving as the physical observable. The approach relies on suppression of harmonics above the 15th order (H15) of the Ti:sapphire driver laser ($\lambda_L = 0.8\,\mu m$) used in our experiments to avoid single-photon ionization of He and on sufficiently intense lower-order harmonics to induce measurable two-photon ionization.

Suppression of harmonics of order $\geqslant 16$ can be ascertained by using a filter with a sharp edge at a photon energy of $\sim$24.6 eV or inhibiting the emission process itself beyond this energy. In our measurements we have exploited both methods to select XUV harmonics between H8 and H14, by filtering with a 150-nm-thick In foil and by confinement of the emission through the generation process to harmonics below the H14. Owing to the In filter, harmonics H8–H10 are the most intense ones in the transmitted spectrum. The harmonics are reproducibly generated by focusing the 45 fs pulses from ATLAS laser system at the Max-Planck-Institut für Quantenoptik (see Methods section) onto a BK7-glass (density $\sim 2.6\ g\,cm^{-3}$) or a polymethylmethacrylate (PMMA) (density $\sim 1.2\ g\,cm^{-3}$) target under 45° angle of incidence (Fig. 1). The spatially averaged, effective laser intensity on target is estimated as $I_L \simeq 4\times10^{18}\ W\,cm^{-2}$, yielding a normalized amplitude of $a_L \simeq 1.5$ for $\lambda_L = 0.8\,\mu m$. At this intensity, both mechanisms discussed above may play a role in the XUV harmonic generation.

However, the appearance of a distinct cut-off in the harmonic emission spectra and the scaling of this cut-off with target density (Fig. 2) suggest that the CWE mechanism provides a dominant contribution in our experiments. In fact, CWE was found to show a well-defined cut-off that moves to higher energy for increasing density[15,18] (see Supplementary Information) as can be seen by comparing the spectra in Fig. 2a,c with those in Fig. 2b,d. The cut-off showing up at H14 for the low-density source corresponds to the maximum resonance frequency that can be supported by the plasma density of this material. This fortuitous circumstance, due mainly to the CWE generation mechanism, is most helpful in suppressing single-photon ionization of the He atoms, which is induced by H16 and higher orders emerging from the high-density source (Fig. 2). As a consequence, we are able to produce a clean two-photon-induced He^+ ion signal with the XUV harmonics from the low-density source, as demonstrated by the approximately quadratic scaling of the ion signal with XUV intensity. In clear contrast to this, the ion signal produced with the XUV beam from the high-density source shows a nearly linear intensity scaling, indicating the dominance of single-photon induced transitions in the ionization. Hence the XUV harmonic emission produced from the low-density source and filtered with an In foil (see Fig. 2a) constitutes an ideal prerequisite for the nonlinear AC experiment.

The temporal characterization of the superposition of harmonics shown in Fig. 2a was performed in two steps. The overall duration of the XUV emission is obtained by a coarse scan (delay step size 3.3 fs)

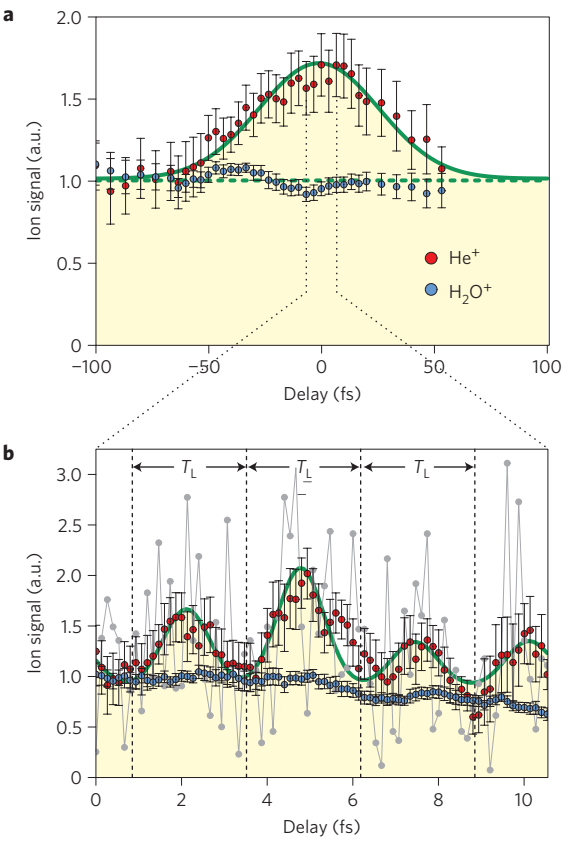

Figure 3 | Measured nonlinear volume AC of the coherent XUV beam comprising H8–H14 from low-density targets. The data are obtained from the He^+ and H_2O^+ ion signal in the mass spectra by varying the delay between the two parts of the split mirror. The moving averages of the raw data taken over nine delay points are shown, with the error bars representing one standard error of the mean. The red circles represent the He^+signal produced by two-photon ionization whereas the blue circles the single-photon ionization of H_2O. The H_2O^+ signal level relative to the He^+ signal is scaled arbitrarily. **a**, A coarse scan over the laser pulse duration (delay step 3.3 fs). A Gaussian fit to He^+ raw data (green line) yields a duration for the XUV emission $T_{XUV} = 44 \pm 20$ fs. **b**, A fine scan near zero delay with a delay step size of 133 as ($\sim$20 data points per laser cycle). The raw data are shown as grey circles connected by grey lines. The green line is a fit to the raw data (grey circles) of a sequence of Gaussian pulses to the second-order XUV AC signal yielding $\tau_{XUV} = 0.9 \pm 0.4$ fs. In both panels, the H_2O^+ signal serves as reference for monitoring the XUV intensity and provides a clear indication of the absence of modulation as a result of single-photon ionization.

of the ion signal as a function of the delay between the two replicas of the XUV pulse prepared by the split mirror for the AC (Fig. 1). From the resultant AC trace shown in Fig. 3a we evaluate an overall duration of the XUV emission as the full-width at half-maximum (FWHM) of the envelope of the XUV emission assuming a Gaussian profile, which gives $T_{XUV} \approx 44 \pm 20$ fs. The fact that this value is very close to the laser pulse duration indicates that CWE scales nearly linearly with laser intensity, which agrees with the findings in ref. 15. To ascertain whether the XUV emission shows a sub-laser-cycle temporal structure indicative of attosecond synchronism among the filtered harmonics, we have performed a fine scan (delay step size 0.13 fs) over a delay interval of ~4 laser cycles centred near the zero delay that yielded the maximum signal in the coarse scan. Figure 3b shows the result of this fine scan. A quasiperiodic subfemtosecond structure with the period of the driving laser field, T_L, is clearly discernible. This is in contrast to the time structure of atomic harmonics, which is characterized by a pulse spacing of $T_L/2$ due to the absence of even harmonics in the emission spectrum. Fitting a train of Gaussian pulses to the measured AC trace gives an estimate for the duration of the individual pulses of $\tau_{XUV} \approx 0.9 \pm 0.4$ fs FWHM. This is the first observation of a subfemtosecond pulse train in the emission emanating from a laser–plasma interaction.

The Fourier limit of the pulses that can be synthesized with the filtered harmonic composition is ~0.5 fs. One possible physical reason for the deviation from this value is the existence of chirp. The presence of a chirp in the emitted subfemtosecond bursts is consistent with our previous finding that CWE is the dominant mechanism responsible for XUV emission. As explained in Supplementary Information, the CWE harmonics possess an intrinsic 'atto chirp' and equation (1) predicts for the superposition of the seven harmonics experimentally selected and for estimated plasma scale lengths in the range of $L/\lambda = 0.1$–0.5 the emergence of chirped pulses with durations of 0.8–1 fs, in plausible agreement with the experimental data. The accuracy of the measurements however does not allow the definite identification of the source of broadening, and other factors that can contribute to it cannot be excluded. The question concerning the atto chirp of the harmonic emission has to be investigated in more accurate measurements using higher laser intensities. Information thus acquired might reveal superior phase-locking properties associated with the ROM harmonic generation mechanism, as the analysis presented in Supplementary Information presages (see Supplementary Information, Fig. S2).

In summary, our work provides experimental evidence for the phase synchronism of XUV plasma harmonics required for attosecond light bunching. The result motivates advancement of multiterawatt few-cycle laser technology[28], particularly in providing sufficiently high-contrast laser pulses as an alternative to the use of plasma mirrors[16,17]. This will lead to isolated subfemtosecond pulses with peak intensities rivalling those produced by accelerator-based sources[5]. Powerful attosecond pulses from few-cycle-driven overdense plasmas will provide access to correlated intra-atomic electron motion through XUV pump–probe spectroscopy[29] and—with scaling of the laser pulse energy—to unprecedented field strengths[30], holding promise for advancing time-resolved and high-field science likewise.

Methods

Experimental set-up. The ATLAS facility of the Max-Planck-Institut für Quantenoptik, a Ti:sapphire CPA system, has delivered ~700 mJ, 45-fs-FWHM pulses at 10 Hz for the experiments. Its 60-mm-diameter *p*-polarized laser beam was focused by a 30° dielectric-coated optical-quality-polished off-axis parabolic mirror with 160 mm focal length at 45° angle of incidence onto a rotating disc-shaped target (polished BK7-glass or PMMA substrates of 12 cm in diameter) (see Fig. 1). Focusing the beam results in a peak intensity of $\sim 4 \times 10^{19}$ W cm^{-2} on the optical axis, whereas a careful analysis of the experimental record yields a spatially averaged intensity (over the $1/e^2$ radius containing 86% of the energy) of $\sim 4 \times 10^{18}$ W cm^{-2}. This average intensity, corresponding to an effective normalized amplitude of $a_L \sim 1.5$, is more pertinent to the experiment because the CWE process is nearly linear in intensity. Third-order AC of the laser pulse yields an intensity contrast of $\sim 10^8$ 4 ps in front of the pulse peak. The disc-shaped targets are mounted on a rotational–translational stage, enabling target-area replenishment with high precision at a rate sufficient for 10 Hz operation. One disc can be exposed to about 5,000 laser shots before replacement.

Extreme-ultraviolet beam characterization. The selection of the harmonic composition necessary for XUV AC is accomplished by proper choice of target and thin-film materials. The maximum plasma density available during the interaction with low-density targets (PMMA) is estimated as $n_{e,max}^{\text{low density}}/n_c \approx 200$. This yields a maximum harmonic order of $q_{max}^{\text{low density}} \approx \sqrt{200} \approx 14$. The corresponding cut-off harmonic for high-density (BK7-glass) targets is $q_{max}^{\text{high density}} \approx \sqrt{400} = 20$ because $n_{e,max}^{\text{high-density}}/n_c \approx 400$. Thus, the combination of low-density targets and an In filter results in a harmonic composition consisting of harmonics H8–H14. This ensures sufficient suppression of harmonics higher than H15 that can cause single-photon ionization of He.

The laser-to-XUV conversion efficiency for the spectral range thus selected was estimated by measuring the XUV energy at the split mirror using a calibrated XUV photodiode. Taking into account all losses introduced in the path between the plasma source and the split mirror (recollimating parabolic mirror reflection, SiO_2 plate reflection and In filter transmission), which are of the order of $\sim 10^3$, leads to a conservative estimate of $\eta_{XUV} \geqslant 6 \times 10^{-5}$ for the laser-to-XUV conversion efficiency at the source. We have estimated (with the help of ray tracing) the XUV beam diameter at the focus of the split mirror to be about ~10 μm, yielding thus an XUV intensity at the interaction region of $I_{XUV} \simeq (0.5\text{–}1) \times 10^{11}$ W cm^{-2}. Also, a detailed study of the focal region similar to the one presented in ref. 25 with variation of the spacing between the two parts of the split mirror has been performed to ascertain the signal-to-background ratio of the volume AC signal under realistic conditions (XUV beam diameter of 25 mm and 8° angle between the incoming and outgoing beams). The relatively large tilt angle introduces some aberrations in the focus, with the consequence that the expected signal-to-background ratio is ~1.5:1 under our experimental conditions. This is in rough agreement with the experimentally observed signal-to-background ratio (see Fig. 3).

Extreme-ultraviolet AC data acquisition and analysis. The He^+ ion yield was recorded by a time-of-flight mass spectrometer. The ionization occurs through two-XUV-photon non-resonant absorption from all possible combinations of the selected set of harmonics. By piezoelectrically varying the delay between the two halves of the split mirror, the spatial distribution of the XUV intensity in the focal region is changed. Although the total energy remains the same, this intensity variation due to interference of all harmonics for a particular delay allows for second-order AC measurements. For the coarse and fine scans, the mass spectra were obtained by accumulating 20 shots at each delay value and taking their average. The mass spectra thus recorded were stored for further analysis in an array of ~80 delay steps, representing approximately 1600 shots in the fine scan.

The He^+ signal in the coarse as well as in the fine scan represents the second-order AC of the two delayed XUV pulses. To make the trend of AC clearer, the moving averages of the raw data are taken over nine delay points and shown in Fig. 3 with the error bars representing one standard error to the mean. For the case of the coarse scan, a Gaussian fit to He^+ raw data (green line) yields the overall duration of the XUV emission $T_{XUV} = 44 \pm 20$ fs FWHM. For the H_2O^+ a straight line fit is used (green dashed line). In the case of the fine scan, a fit to the raw data (grey points) of five Gaussians with background was performed (green line). The constraints imposed on the fit were that (1) the interval between the peaks was kept equal to the laser period, 2.67 fs, and (2) all five Gaussians have the same but variable width. The other parameters such as amplitude of each peak and background level were free to vary. This gives an estimate for the subfemtosecond pulse duration as $\tau_{XUV} \approx 0.9 \pm 0.4$ fs FWHM.

The effect of the smoothing over nine delay points (red and blue circles) on the AC signal duration τ_0 (FWHM) can be estimated using the expression $\tau_1^2 \approx \tau_0^2 + \tau_F^2$ (strictly valid for the convolution of two Gaussians), where τ_F is the width of the smoothing function and τ_1 the resulting width after smoothing. (The XUV pulse durations have been estimated from the AC signal durations using the approximation $\tau_{XUV} \approx \tau_0/\sqrt{2}$.) In the case of the coarse scan for $\tau_0 \approx 62.2$ fs (deduced from the fit to the raw data) and $\tau_F \approx 8 \times 3.3 = 26.4$ fs we obtain $\tau_1 \approx 67.6$ fs. This represents less than 10% difference, and as consequence the fitted curve and the smoothed signal are almost indistinguishable. The corresponding values for the case of the fine scan are $\tau_0 \approx 1.3$ fs (again deduced from the fit to the raw data) and $\tau_F \approx 8 \times 0.13 = 1.04$ fs, thus $\tau_1 \approx 1.7$ fs. Here the effect is larger (about 30%), but given the large error bars associated with the smoothed data the difference between the fitted curve and the smoothed data is barely discernible. For the same reason, the change in the signal-to-background ratio after smoothing is not substantially affected.

Received 6 June 2008; accepted 10 November 2008; published online 14 December 2008

References

1. Goulielmakis, E. *et al.* Single-cycle nonlinear optics. *Science* **320**, 1614–1617 (2008).
2. Sansone, G. *et al.* Isolated single-cycle attosecond pulses. *Science* **314**, 443–446 (2006).
3. Drescher, M. *et al.* Time-resolved atomic inner-shell spectroscopy. *Nature* **419**, 803–807 (2002).
4. Cavalieri, A. L. *et al.* Attosecond spectroscopy in condensed matter. *Nature* **449**, 1029–1032 (2007).
5. Ackermann, W. *et al.* Operation of a free-electron laser from the extreme ultraviolet to the water window. *Nature Photon.* **1**, 336–342 (2007).
6. Bulanov, S. V., Naumova, N. M. & Pegoraro, F. Interaction of an ultrashort, relativistically strong laser pulse with an overdense plasma. *Phys. Plasmas* **1**, 745–757 (1994).
7. Lichters, R., Meyer-ter-Vehn, J. & Pukhov, A. Short-pulse laser harmonics from oscillating plasma surfaces driven at relativistic intensity. *Phys. Plasmas* **3**, 3425–3437 (1996).
8. Plaja, L., Roso, L., Rzążewski, K. & Lewenstein, M. Generation of attosecond pulse trains during the reflection of a very intense laser on a solid surface. *J. Opt. Soc. Am. B* **15**, 1904–1911 (1998).
9. Naumova, N. M., Nees, J. A., Sokolov, I. V., Hou, B. & Mourou, G. A. Relativistic generation of isolated attosecond pulses in a λ^3 focal volume. *Phys. Rev. Lett.* **92**, 063902 (2004).
10. Gordienko, S., Pukhov, A., Shorokhov, O. & Baeva, T. Relativistic Doppler effect: Universal spectra and zeptosecond pulses. *Phys. Rev. Lett.* **93**, 115002 (2004).
11. Tsakiris, G. D., Eidmann, K., Meyer-ter-Vehn, J. & Krausz, F. Route to intense single attosecond pulses. *New J. Phys.* **8**, 19 (2006).
12. Baeva, T., Gordienko, S. & Pukhov, A. Theory of high-order harmonic generation in relativistic laser interaction with overdense plasma. *Phys. Rev. E* **74**, 046404 (2006).
13. Rykovanov, S. G., Geissler, M., Meyer-ter-Vehn, J. & Tsakiris, G. D. Intense single attosecond pulses from surface harmonics using the polarization gating technique. *New J. Phys.* **10**, 025025 (2008).
14. Tarasevitch, A. *et al.* Generation of high-order spatially coherent harmonics from solid targets by femtosecond laser pulses. *Phys. Rev. A* **62**, 023816 (2000).
15. Quéré, F. *et al.* Coherent wake emission of high-order harmonics from overdense plasmas. *Phys. Rev. Lett.* **96**, 125004 (2006).
16. Dromey, B. *et al.* High harmonic generation in the relativistic limit. *Nature Phys.* **2**, 456–459 (2006).
17. Thaury, C. *et al.* Plasma mirrors for ultrahigh-intensity optics. *Nature Phys.* **3**, 424–429 (2007).
18. Tarasevitch, A., Lobov, K., Wünsche, C. & von der Linde, D. Transition to the relativistic regime in high order harmonic generation. *Phys. Rev. Lett.* **98**, 103902 (2007).
19. Dromey, B. *et al.* Bright multi-keV harmonic generation from relativistically oscillating plasma surfaces. *Phys. Rev. Lett.* **99**, 085001 (2007).
20. Farkas, Gy. & Tóth, Cs. Proposal for attosecond light pulse generation using laser induced multiple-harmonic conversion processes in rare gases. *Phys. Lett. A* **168**, 447–450 (1992).
21. Agostini, P. & DiMauro, L. F. The physics of attosecond light pulses. *Rep. Prog. Phys.* **67**, 813–855 (2004).
22. Quéré, F. *et al.* Phase properties of laser high-order harmonics generated on plasma mirrors. *Phys. Rev. Lett.* **100**, 095004 (2008).
23. Hinkel-Lipsker, D. E., Fried, B. D. & Morales, G. J. Analytic expression for mode conversion of Langmuir and electromagnetic waves. *Phys. Rev. Lett.* **62**, 2680–2682 (1989).
24. Kobayashi, Y., Sekikawa, T., Nabekawa, Y. & Watanabe, S. 27-fs extreme ultraviolet pulse generation by high-order harmonics. *Opt. Lett.* **23**, 64–66 (1998).
25. Tzallas, P., Charalambidis, D., Papadogiannis, N. A., Witte, K. & Tsakiris, G. D. Direct observation of attosecond light bunching. *Nature* **426**, 267–271 (2003).
26. Nabekawa, Y. *et al.* Conclusive evidence of an attosecond pulse train observed with the mode-resolved autocorrelation technique. *Phys. Rev. Lett.* **96**, 083901 (2006).
27. Nikolopoulos, L. A. A. *et al.* Second order autocorrelation of an XUV attosecond pulse train. *Phys. Rev. Lett.* **94**, 113905 (2005).
28. Tavella, F. *et al.* Dispersion management for a sub-10-fs, 10 TW optical parametric chirped-pulse amplifier. *Opt. Lett.* **32**, 2227–2229 (2007).
29. Hu, S. X. & Collins, L. A. Attosecond pump probe: Exploring ultrafast electron motion inside an atom. *Phys. Rev. Lett.* **96**, 073004 (2006).
30. Gordienko, S., Pukhov, A., Shorokhov, O. & Baeva, T. Coherent focusing of high harmonics: A new way towards the extreme intensities. *Phys. Rev. Lett.* **94**, 103903 (2005).

Acknowledgements

This work was supported in part by DFG-Project Transregio TR18, by The Munich Centre for Advanced Photonics (MAP), by the European Community's Human Potential Programme under contract MRTN-CT-2003-505138 (XTRA) and MTKD-CT-2004-517145 (X-HOMES), by the FP6 project 'Laserlab-Europe', contract RII3-CT-2003-506350, and by the Association EURATOM—Max-Planck-Institut für Plasmaphysik.

Additional information

Supplementary Information accompanies this paper on www.nature.com/naturephysics. Reprints and permissions information is available online at http://npg.nature.com/reprintsandpermissions. Correspondence and requests for materials should be addressed to G.D.T.

Supplementary Information

SUPPLEMENTARY DISCUSSION for:

Attosecond phase locking of harmonics emitted from laser-produced plasmas

Y. Nomura*[1], R. Hörlein*[1,2], P. Tzallas[3], B. Dromey[5], S. Rykovanov[1,6], Zs. Major[1], J. Osterhoff[1], S. Karsch[1], L. Veisz[1], M. Zepf[5], D. Charalambidis[3,4], F. Krausz[1,2], & G. D. Tsakiris[1]

[1]*Max-Planck-Institut für Quantenoptik, Hans-Kopfermann-Str. 1, D-85748 Garching, Germany*

[2]*Department für Physik, Ludwig-Maximilians-Universität, Am Coulombwall 1, D-85748 Garching, Germany*

[3]*Foundation for Research and Technology - Hellas, Institute of Electronic Structure & Laser, PO Box 1527, GR-711 10 Heraklion (Crete), Greece*

[4]*Department of Physics, University of Crete, P.O. Box 2208, GR-71003 Voutes-Heraklion (Crete), Greece*

[5]*Department of Physics and Astronomy, Queens University Belfast, BT7 1NN, UK*

[6]*Moscow Physics Engineering Institute, Kashirskoe shosse 31, 115409 Moscow, Russia*

The answer to the question whether the harmonic emission from solid targets interacting with intense laser pulses are Fourier transformed limited (FTL) or possess an intrinsic chirp has to be sought in the details of the generation mechanism. As in the case of atomic harmonics, we distinguish here between the chirp among harmonics (atto chirp) and the chirp within the individual harmonics (harmonic chirp)[31]. The first chirp

results in broadening of the individual attosecond pulses while the second in the broadening of the overall XUV emission envelope. In case of harmonic from solid targets, contributions to the atto chirp come from non-concomitant harmonic sources, while to the harmonic chirp, similarly to the case of atomic harmonics, from deviation in the periodicity of appearance of the attosecond pulses. The two harmonic generation mechanisms of coherent wake emission (CWE) and relativistic oscillating mirror (ROM) are quite different in origin and therefore apt to contribute to a different degree to the chirping.

To understand the origin of the chirps in the CWE harmonics, the generation process is schematically depicted in Fig. SI-1. The orbits of the fast electrons responsible for the density fluctuations in the plasma ramp are shown to differ due to the varying amplitude of each cycle under the laser pulse envelope. The disparity in the re-entry time of the electrons causes a variation in the periodicity of the appearance of the individual attosecond pulses[22] (harmonic chirp). However, this represents a temporal chirp which results in spectral broadening of the harmonics. The temporal broadening of the individual attosecond pulse is due to the fact that higher-order harmonics are generated deeper in the plasma density profile, where the plasma density is higher, and thus travel longer than the lower-order harmonics (atto chirp). This scenario is corroborated by the results of PIC simulations with parameters close to experimental ones and a linear spatial density profile with scale length $L = 0.2\lambda$ (here defined as the length over which the electron density increases from zero to solid density), shown also in Fig. SI-1. This plasma ramp scale length corresponds to the optimum value for harmonic generation by p-polarized light incident at 45° angle[32]. Furthermore, for this scale length and the laser intensity considered the dominant absorption mechanism is vacuum heating[33,34]. The Fourier analysis of the current component perpendicular to the interface j_x shows a localization of the nonlinear currents at particular positions within the density ramp[18,35]. The source of the q^{th}-order harmonic is seen to be located along a

parabolic profile at the position x_q where the density supports the corresponding resonance, i.e., where $n_e(x_q) = n_c\omega_p^2(x_q)/\omega_L^2 = n_c q^2$. Despite the fact that the various frequency components are coherently excited, they travel different distances from the source giving rise to a chirped attosecond pulse. The amount of the atto chirp can be estimated with a simple model assuming a linear density profile. If the electrons are assumed to travel at the speed of light and the refractive index in the plasma is taken into account, for 45º angle of incidence the phase accumulated by the q^{th} harmonic representing the atto chirp is calculated as

$$\varphi_q = \frac{5\sqrt{2}}{3}\frac{n_e(x_q)}{n_{e,\max}}k_q L \propto q^3, \qquad (1)$$

where k_q is the wave number of the q^{th} harmonic. In deriving this expression, the phase ϕ_q accumulated by the q-th harmonic is calculated as the sum of the time needed by the electrons to travel to a given depth and that for each harmonic to emerge into the vacuum.

The second generation mechanism of ROM dominates at relativistic intensities, i.e. when $a_L^2 \gg 1$. The underlying physics is the relativistic Doppler frequency shift of an EM-wave back-reflected by a surface moving at velocities close to the speed of light. The interaction of intense laser pulses with plasma results in forced oscillations of the electrons bound to the slowly moving ions. When the laser pulse is reflected by these electrons, it undergoes a frequency up-shift and a spectrum is generated encompassing frequencies up to the roll-over frequency $\omega_{RO}^{ROM} \propto \gamma_{max}^3\omega_L$ where $\gamma_{max} \approx a_L$ for $a_L \gg 1$ is the relativistic Lorentz factor. In this simplified picture of the ROM mechanism, intuitively one expects the harmonics to carry an atto chirp because the reflection occurs at different times and speeds, which results in a time-varying Doppler upshift,. However, as it has been pointed out by Baeva *et al.*[12], the emission occurs in the neighbourhood of the so-called relativistic γ-spikes, the width of which varies as $1/\gamma_{max}$.

At high intensities giving rise to high values of γ_{max}, these γ-spikes tend to be very narrow in time and symmetric so that no appreciable chirp contribution arises. This picture is supported by a detailed analytical treatment, which shows that the phases of the harmonic emission are proportional to the harmonic order[12]. In case of ROM harmonics, as is discussed in Ref. 22, the harmonic chirp is negligible.

To verify the difference in the atto chirp associated with each of the two generation mechanisms, we have performed simulations with 1D PIC code[13] for two cases, for $a_L = 0.2$ and $a_L = 10$. These two cases were judiciously chosen in a way that one represents the CWE ($a_L \ll 1$) and the other the ROM ($a_L \gg 1$) mechanism. To visualize the chirp of the harmonic emission, we have post-processed the simulation results by performing a wavelet analysis[13,36,37]. The frequency-time diagram for each case along with the reflected field and the resulting attosecond pulse train are shown in Fig. SI-2. It is clearly seen that the low intensity case ($a_L = 0.2$) where CWE generation mechanism is effective exhibits a substantial chirp manifested by the inclination of the harmonics with respect to the time axis. In contrast, the harmonic for high intensities ($a_L = 10$) where the ROM mechanism is dominant appear to be chirp-free. It is also observed that the same harmonic composition (H8 to H14) in the two cases produces attosecond pulses of different duration. The fact that the high-intensity case yields shorter pulses indicates that the attosecond pulses in the low-intensity case carry a frequency chirp.

References

31. Varjú, K. *et al.* Frequency chirp of harmonic and attosecond pulses. *J. Mod. Opt.* **52**, 379 (2005).

32. Eidmann, K. *et al.* Fundamental and harmonic emission from the rear side of a thin overdense foil irradiated by an intense ultrashort laser pulse. *Phys. Rev. E* **72**, 036413 (2005).

33. Brunel, F. Not-So-Resonant, Resonant Absorption. *Phys. Rev. Lett.* **59**, 52 (1987).

34. Cerchez, M. *et al.* Absorption of Ultrashort Laser Pulses in Strongly Overdense Targets. *Phys. Rev. Lett.* **100**, 245001 (2008).

35. Teubner, U. *et al.* Harmonic Emission from the Rear Side of Thin Overdense Foils Irradiated with Intense Ultrashort Laser Pulses. *Phys. Rev. Lett*. **92**, 185001 (2003).

36. Goupillaud, P., Grossmann, A. & Morlet, J. CYCLE-OCTAVE AND RELATED TRANSFORMS IN SEISMIC SIGNAL ANALYSIS. *Geoexploration* **23**, 85 (1984).

37. Pirozhkov, A. S. *et al.* Attosecond pulse generation in the relativistic regime of the laser-foil interaction: The sliding mirror model. *Phys. Plasmas* **13**, 013107 (2006).

Figure SI-1: Schematic and PIC simulations to elucidate the origin of the chirps inherent in the CWE generation mechanism. In the upper diagram, the electron orbits are schematically shown to enter the plasma density ramp at different times depending on the amplitude of the electric field in the laser pulse. This results in broader harmonics. The actual atto chirp is due to the de-localization of the individual harmonic source within the plasma ramp. This is confirmed by the results of the 1D-PIC simulations shown in the lower panel. They were conducted with parameters of $a_L = 1.5$, 45° angle of incidence, and Gaussian pulse envelope of 15 laser cycles. A ramp of $L = 0.2\lambda$ scale-length was assumed to exist in front of the plasma. The maximum electron density was taken to be $n_{e,\max} = 200 n_c$, which corresponds to the density of the low density target material (PMMA). The colour plot shows current component j_x perpendicular to the target normalized to the maximum value and in logarithmic scale as a function of frequency and space. It is seen that the harmonics of the current are localized inside the density ramp along a parabola defined by the relation $\omega_q(x) = \omega_L \sqrt{n_e(x)/n_c}$, i.e., at positions where the local plasma frequency is in resonance with a given harmonic. The frequency cutoff at the 14th harmonic determined by the maximum electron density is also clearly seen. The difference in distance in the plasma gradient of each harmonic gives rise to the atto chirp.

Figure SI-2: PIC simulations results for a low $a_L = 0.2$ (panels (a) and (b)) and a high $a_L = 10.0$ (panels (c) and (d)) intensity case. The simulations were performed with 1D PIC code for the following parameters: laser pulse duration 15 laser cycles, 45° angle of incidence, plasma density 200 overcritical, linear plasma density ramp with scale length $L = 0.2\lambda$ and for mobile ions. Panels (a)

and (c) show on a linear scale the results of the wavelet analysis of the emission, while panels (b) and (d) the total reflected *E*-field (blue line) and the instantaneous intensity of the resulting attosecond pulse train composed of H8 to H14 (red line). The spread of the emission over time of the different harmonics in the range H8 to H14 (inclination denoted by dotted line) in the low intensity case (panel (a)) is a clear indication of atto chirp. In contrast, the high intensity case for the same harmonic range exhibits no discernible atto chirp (panel (c)). As a consequence, the individual attosecond pulse duration differs considerably between the two cases, with the high intensity case delivering shorter pulses.

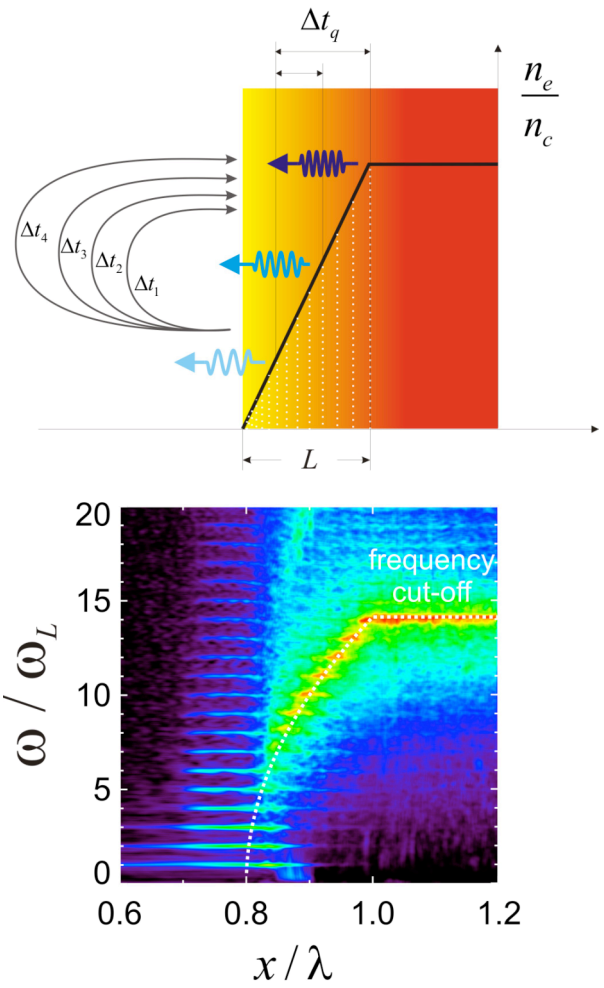

Fig. SI-1 “Attosecond phase locking of harmonics …” by Y. Nomura *et al.*

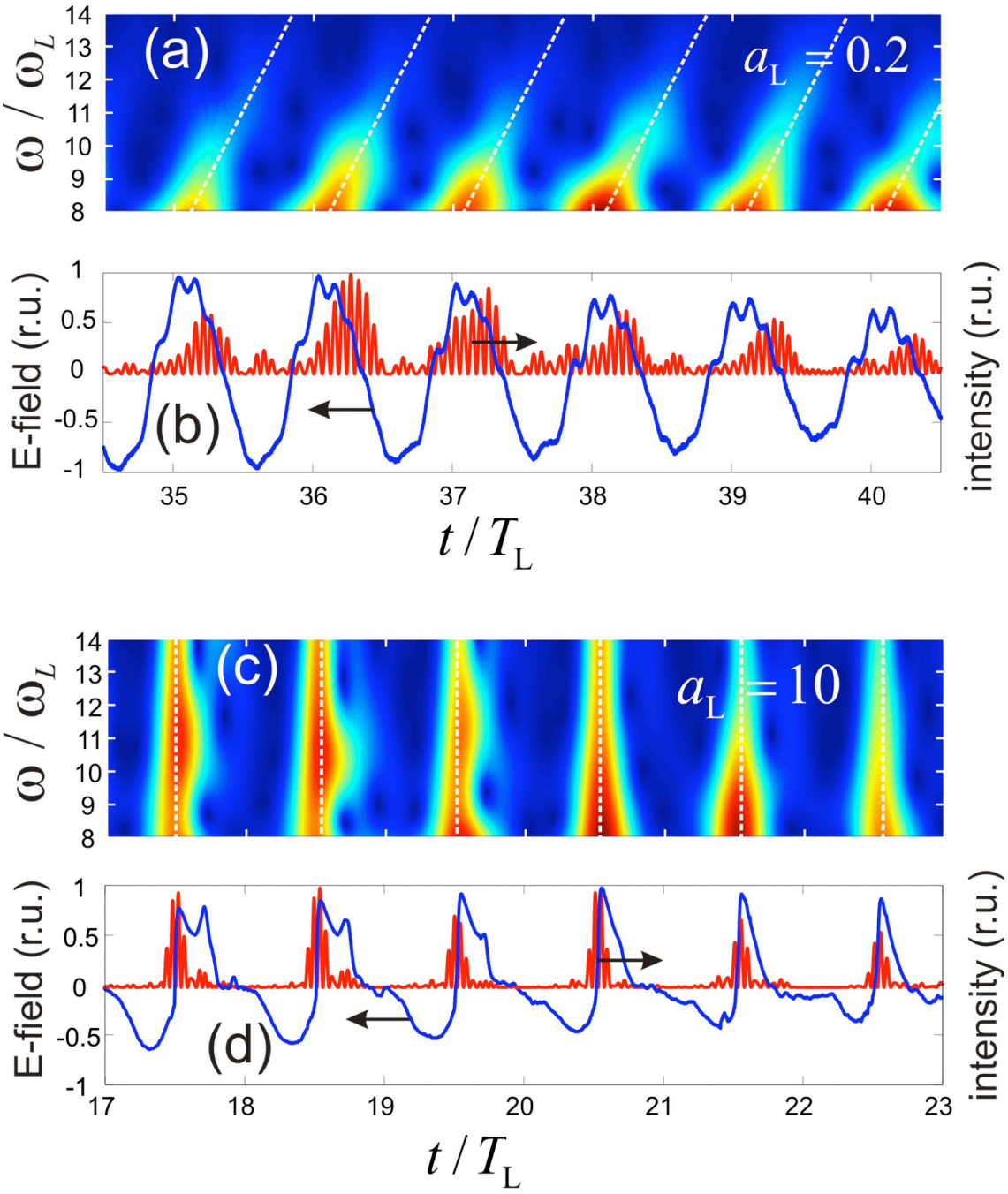

Fig. SI-2 "Attosecond phase locking of harmonics …" by Y. Nomura *et al.*

smaller than the electron thermal-energy density. However, the kinetic theory can be further generalized for the high-frequency elliptically polarized extraordinary electromagnetic wave, propagating transverse to the external magnetic field, with the spin-modified anisotropic Fermi–Dirac distribution function.

It is worth considering the implications of collective interactions in dense quantum plasmas that have quantum and spin forces. Collective interactions in quantum plasmas are truly interdisciplinary — they combine quantum mechanics, plasma physics, fluid dynamics, condensed matter and statistical physics. The potential for using spin in practical applications has already been realized in a number of different fields (the award of the 2007 Nobel Prize in Physics to Albert Fert and Peter Grünberg for their work on giant magnetoresistance is just one example). It is hoped that the field of quantum plasmas will also find practical applications in the production of localized X-ray sources, quantum free-electron lasers[8,9] and plasma-assisted microelectronic components. Also, a better understanding of the role of electron spin in quantum plasmas may aid the development of intense-laser-beam compression for controlled nuclear fusion. ❐

Padma Kant Shukla is in the Faculty of Physics and Astronomy, Ruhr University Bochum, D-44780 Bochum, Germany.
e-mail: ps@tp4.rub.de

References

1. Brodin, G., Marklund, M., Zamanian, J., Ericsson, A. & Mana, P. L. *Phys. Rev. Lett.* **101,** 245002 (2008).
2. Harding, A. K. & Lai, D. *Rep. Prog. Phys.* **69,** 2631–2708 (2006).
3. Glenzer, S. H. *et al. Phys. Rev. Lett.* **98,** 065002 (2007).
4. Gardner, C. L. & Ringhofer, C. *Phys. Rev. E* **53,** 157–167 (1996).
5. Manfredi, G. *Fields Inst. Commun.* **46,** 263–287 (2005).
6. Shukla, P. K. & Eliasson, B. *Phys. Rev. Lett.* **96,** 245001 (2006).
7. Brodin, G. & Marklund, M. *Phys. Rev. E* **76,** 055403(R) (2007).
8. Piovella, N. *et al. Phys. Rev. Lett.* **100,** 044801 (2008).
9. Serbeto, A., Mendonça, J. T., Tsui, K. H. & Bonifacio, R. *Phys. Plasmas* **15,** 013110 (2008).

ULTRAFAST SCIENCE

Attosecond plasma optics

Using dense plasmas instead of atomic or molecular gases could enable the generation of attosecond light pulses with higher energy, shorter durations and more energetic photons.

Fabien Quéré

Ultrashort light pulses can temporally resolve the evolution of dynamical systems such as excited molecules. Resolving faster and faster processes obviously requires shorter and shorter light pulses. Pulses with durations in the attosecond range (1 as = 10^{-18} s) — short enough to start resolving the dynamics of electrons in matter — can be generated and measured[1] by exploiting laser–atom or laser–molecule interactions. However, applications of these pulses have been hindered by limits to pulse and photon energies. On page 124 of this issue[2], Yutaka Nomura and colleagues demonstrate experimentally a new kind of attosecond light source that might eventually push these limits by taking advantage of ultrahigh-intensity laser–plasma interactions.

For more than twenty years, laser technology has exploited the chirped-pulse amplification technique to produce intense light pulses that only last a few tens of femtoseconds. Fifteen years ago, these pulses were identified theoretically as a promising tool for obtaining even shorter pulses — potentially of attosecond duration[3,4]. The basic idea is to make such a pulse interact with a system at high intensity, so that its waveform is temporally distorted by the nonlinear response of the system. Because this distortion generally has the same periodicity as the driving laser, the spectrum of the resulting light field consists of a comb of harmonics of the incident frequency. For a severe distortion, these harmonics reach very high orders, thus leading to a very broad spectrum — a prerequisite for very short pulses. If this distortion is temporally localized within each laser optical cycle — or, equivalently, if the harmonics making up the spectrum are approximately in phase — a train of sub-laser-cycle pulses can then be obtained simply by filtering out the fundamental frequency and selecting a group of harmonics in the spectrum.

Distortions of the laser-field waveform have so far been achieved by exploiting a process called laser-driven electron–ion recollision[1]. Electron wavepackets are periodically freed from a target atom or molecule by tunnel ionization. Part of these wavepackets return to their parent

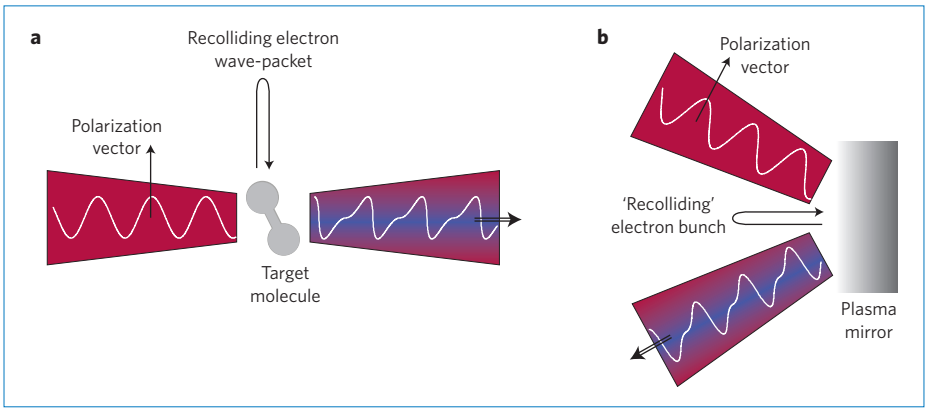

Figure 1 | Working in analogy. **a**, Laser-driven electron–ion recollision can create attosecond pulses. An input laser (red wave) frees an electron wave-packet from a target atom or molecule. An attosecond light pulse is generated when part of this wave-packet returns to the ion. **b**, Excitation lasers of much higher intensity create a plasma. Nomura *et al.*[2] show experimentally that this can generate attosecond pulses in much the same way. At even higher intensities, the Doppler effect induced as the laser beam reflects on the plasma has the potential to generate attosecond pulses with a shorter duration and with higher energy photons.

ion after having gained energy during their excursion in the continuum. This energy can be released in the form of an attosecond light pulse, emitted as the recolliding wavepacket overlaps and interferes with the remaining population in the initial ground state, thus creating a high-frequency dipole (Fig. 1a).

The maximum frequency generated in this interaction, and hence the shortest pulse duration that can potentially be obtained, are directly related to the maximum energy of the free electrons. This in turn is determined by the laser intensity. However, this delicate recollision process does not survive laser intensities that are too high. The fundamental reason for this is that at intensities approaching 10^{18} W cm^{-2} for a near-infrared field, the motion of electrons in the field becomes relativistic. The effect of the laser magnetic field can then no longer be neglected, and the associated force induces a drift of the electrons along the direction of laser propagation, preventing them from recolliding with their parent ions. Attosecond light sources based on laser-driven electron–ion recollision are therefore intrinsically restricted to intensities much lower than those produced by modern ultrafast, ultra-intense lasers, which commonly exceed this relativistic threshold by several orders of magnitude.

At these so-called relativistic intensities, all targets are rapidly ionized by the leading edge of the laser pulse, creating a plasma. These are generally considered as unstable and uncontrollable media — unlikely to produce coherent light. However, this is not necessarily the case when ultrashort laser pulses are involved. In particular, when such a pulse hits an optically polished surface it generates a dense reflective plasma that only has time to expand by a small fraction of the light wavelength. Thus, it behaves as a highly flat mirror — a plasma mirror. Such plasma mirrors can be used to generate collimated beams of very-high-order harmonics, even at the highest laser intensities[5,6].

According to the theory, these harmonics are associated, in the time domain, with trains of attosecond pulses, like those generated in gases. But this prediction had not been confirmed experimentally — this is precisely what Nomura *et al.*[2] have now done by measuring the nonlinear intensity autocorrelation function of a superposition of several of these harmonics. Because it is an extreme ultraviolet beam, the difficulty was finding a suitable nonlinear effect. Nomura and co-workers' technique relies on two-photon ionization of helium atoms, an approach already demonstrated with gas sources. Its implementation using plasma mirrors, however, is a tour de force. This is particularly the case because of the lower repetition rate required to refresh the target between each shot. Because of large signal fluctuations, these results do not yet provide an accurate temporal characterization of the generated pulses, but by setting an upper limit on their duration, they show that harmonics generated in this way can indeed have a suitable phase relationship for attosecond pulse generation.

The physics of the process used by Nomura *et al.* to produce these pulses — referred to as coherent wake emission[5,7] (Fig. 1b) — has some strong qualitative analogies with electron–ion recollision in gases. Within each laser cycle, electrons at the sharp plasma surface are pulled out into the vacuum by the laser electric field, before being pushed back towards the target when this field changes sign. This creates extremely short electron bunches, which 'recollide' with the dense plasma where they trigger high-frequency collective electron oscillations in their wake. These oscillations subsequently emit attosecond light pulses.

The maximum frequency of these oscillations is limited by the plasma properties[5,7], and therefore this 'electron–plasma recollision' process is not yet suitable for obtaining higher photon energies or shorter attosecond pulses than is already available from gas targets. Reaching this goal will require increasing the laser intensity even further, sufficiently beyond the relativistic limit, and truly exploiting the relativistic character of the resulting interaction. In this regime, the plasma mirror surface oscillates at the laser frequency with a peak velocity approaching the speed of light. This oscillating mirror induces a large periodic Doppler shift on the reflected light, thus potentially leading to extremely high harmonic orders. Collimated light beams with photon energies of several keV have already been obtained in this way using one of the most intense lasers existing today[6,8]. Measuring the phase relationship of the extreme harmonics produced by such a source remains one of the challenges of attosecond metrology: the technique used by Nomura *et al.*[2] does not apply at these higher frequencies, which can ionize helium with a single photon.

In a more general context, many schemes have now been demonstrated experimentally that put plasmas to work as high-intensity optical elements. Such 'plasma optics' can, for instance, be exploited to further amplify[9] ultra-intense lasers and improve their temporal contrast[5], or to tailor or temporally compress[10] ultrashort pulses down to the few-femtosecond range. By demonstrating the feasibility of a plasma-based attosecond light source, the work of Nomura *et al.* has added an important functionality to these fascinating optical elements. ❐

Fabien Quéré is at CEA, IRAMIS, Service des Photons Atomes et Molécules, F-91191 Gif-sur-Yvette, France.
e-mail: fabien.quere@cea.fr

References

1. Corkum, P. B. & Krausz, F. *Nature Phys.* **3,** 381–387 (2007).
2. Nomura, Y. *et al. Nature Phys.* **5,** 124–128 (2009).
3. Hänsch, T. W. *Opt. Commun.* **80,** 71–75 (1990).
4. Farkas, G. & Toth, C. *Phys. Lett. A* **168,** 447–450 (1992).
5. Thaury C. *et al. Nature Phys.* **3,** 424–429 (2007).
6. Dromey, B. *et al. Nature Phys.* **2,** 456–459 (2006).
7. Quéré, F. *et al. Phys. Rev. Lett.* **96,** 125004 (2006).
8. Dromey, B. *et al. Phys. Rev. Lett.* **99,** 085001 (2007).
9. Ren, J., Cheng, W., Li, S. & Suckewer, S. *Nature Phys.* **3,** 732–736 (2007).
10. Faure J. *et al. Phys. Rev. Lett.* **95,** 205003 (2005).